**EPJ manuscript No.**
(will be inserted by the editor)

# Proton-Antiproton annihilation at 900 MeV/$c$ into $\pi^0\pi^0\pi^0$, $\pi^0\pi^0\eta$ and $\pi^0\eta\eta$

## The Crystal Barrel Collaboration

C. Amsler[13], B.M. Barnett[3a], M. Benayoun[10], S. Bischoff[7], P. Blüm[7], K. Braune[9], T. Case[1], K.M. Crowe[1], T. Degener[2], M. Doser[5], W. Dünnweber[9], D. Engelhardt[7], M.A. Faessler[9], P. Giarritta[13], R.P. Haddock[8], F.H. Heinsius[1b], M. Heinzelmann[13c], A. Herbstrith[7], N.P. Hessey[9], P. Hidas[4], D. Jamnik[9d], H. Kalinowsky[3], P. Kammel[1e], J. Kisiel[5f], E. Klempt[3], H. Koch[2], M. Kunze[2], U. Kurilla[2], M. Lakata[1], R. Landua[5], H. Matthäy[2], C.A. Meyer[11], F. Meyer-Wildhagen[9], L. Montanet[5], R. Ouared[5], K. Peters[2], B. Pick[3], M. Ratajczak[2], C. Regenfus[13], W. Roethel[9], S. Spanier[13g] H. Stöck[2], U. Strohbusch[6], M. Suffert[12], J.S. Suh[3], U. Thoma[3], M. Tischhäuser[7], I. Uman[9], C. Völcker[9], S. Wallis-Plachner[9], D. Walther[2h], U. Wiedner[5i], and K. Wittmack[3]

[1] University of California, LBNL, Berkeley, CA 94720, USA
[2] Universität Bochum, D-44780 Bochum, Germany
[3] Universität Bonn, D-53115 Bonn, Germany
[4] Academy of Science, H-1525 Budapest, Hungary
[5] CERN, CH-1211 Geneva 4, Switzerland
[6] Universität Hamburg, D-22761 Hamburg, Germany
[7] Universität Karlsruhe, D-76021 Karlsruhe, Germany
[8] University of California, Los Angeles, CA 90024, USA
[9] Universität München, D-80333 München, Germany
[10] LPNHE Paris VI, VII, F-75252 Paris, France
[11] Carnegie Mellon University, Pittsburgh, PA 15213, USA
[12] Centre de Recherches Nucléaires, F-67037 Strasbourg, France
[13] Universität Zürich, CH-8057 Zürich, Switzerland

10 April 2001

**Abstract.** The three reactions $\overline{p}p \to \pi^0\pi^0\pi^0$, $\pi^0\pi^0\eta$ and $\pi^0\eta\eta$ in proton-antiproton annihilation in flight at 900 MeV/$c$ are used to search for isoscalar $0^{++}$ and $2^{++}$ mesons in the mass range $1000 - 2000$ MeV, in particular the $f_0(1710)$. The description of both $\pi^0\pi^0\pi^0$ and $\pi^0\eta\eta$ data sets requires an isoscalar tensor resonance decaying into $\pi^0\pi^0$ and $\eta\eta$ with a mass of $(1867 \pm 46)$ MeV and a width of $(385 \pm 58)$ MeV. The ratio of partial widths $\Gamma(\eta\eta)/\Gamma(\pi\pi)$ is $0.27 \pm 0.10$. The analyses of both $\pi^0\pi^0\pi^0$ and $\pi^0\eta\eta$ show no signal for the $f_0(1710)$. The $\pi^0\eta\eta$ data set shows a strong signal of the $f_2'(1525)$ suggesting a large OZI rule violation for tensor meson production in $\overline{p}p$ annihilation. The $\pi^0\pi^0\pi^0$ data set also requires the $f_2(1565)$. The signal for the $f_2(1810)$ reported by earlier experiments is confirmed neither in $\pi^0\pi^0\pi^0$ nor in $\pi^0\eta\eta$. The analysis of $\pi^0\pi^0\eta$ leads to an isovector tensor state decaying into $\pi^0\eta$ with a mass of $(1698 \pm 44)$ MeV and a width of $(265 \pm 55)$ MeV.

## 1 Introduction

An earlier analysis of the $\overline{p}p$ annihilation channels $\pi^0\pi^0\pi^0$, $\pi^0\pi^0\eta$ and $\pi^0\eta\eta$ at rest led to a systematic description of the $\pi^0\pi^0$ and $\pi^0\eta$ $S$-waves below 1500 MeV [1]. However, mesons heavier than about 1600 MeV cannot be produced in $\overline{p}p$ annihilation at rest. This paper presents the analyses of proton-antiproton annihilation in-flight at 900 MeV/$c$, corresponding to a center of mass energy of 2050 MeV, into the three final states $\pi^0\pi^0\pi^0$, $\pi^0\pi^0\eta$ and $\pi^0\eta\eta$ leading to six detected photons. In the final step the two channels $\pi^0\pi^0\pi^0$ and $\pi^0\eta\eta$ were described by a coupled fit.

[a] Now at Rutherford Appleton Laboratory, Chilton, UK
[b] Now at University of Freiburg, Freiburg, Germany
[c] This work is the PhD thesis of M. Heinzelmann
[d] University of Ljubljana, Ljubljana, Slovenia
[e] Now at University of Illinois, Urbana Champaign, USA
[f] University of Silesia, Katowice, Poland
[g] Now at SLAC, Stanford, USA
[h] Now at University of Bonn, Bonn, Germany
[i] Now at Uppsala University, Uppsala, Sweden

The coupled channel analysis of $\pi^0\pi^0\pi^0$, $\pi^0\pi^0\eta$ and $\pi^0\eta\eta$ at rest, together with $\pi\pi$ scattering data, described the $(\pi\pi)_S$ and $(\pi\eta)_S-$waves in the $K$-matrix formalism [1]. The $(\pi\pi)_S-$wave included the $f_0(600)$(previously called $f_0(400-1200)$ or $\sigma$), $f_0(980)$, $f_0(1370)$ and $f_0(1500)$[2]. The $(\pi\eta)_S-$wave description had two poles, the $a_0(980)$ and $a_0(1450)$. The $K\bar{K}$ decay of the $a_0(1450)$ was also observed in the analysis of $K^\pm\pi^\mp K_L$ by Crystal Barrel [3]. However, the Obelix Collaboration prefers in the analysis of $K^\pm K_S\pi^\mp$ a narrow (80 MeV) $a_0(1300)$ [4]. Recently the long-standing ambiguity between $J=0,2$ for the $f_J(1710)$ was solved [5,6]. With spin $J=0$ the controversy arises as whether this scalar state could be the missing $s\bar{s}$ member of the $0^{++}$ nonet, the scalar glueball or a mixing of both [7]. In the tensor sector the $f_2(1565)$, first observed by the Asterix Collaboration [8], needs confirmation in flight as it was only seen in nucleon-antinucleon annihilations at rest. In the available mass range up to 2 GeV there are two other possible isoscalar tensor resonances, the $f_2(1810)$ and $f_2(1950)$, which both need to be confirmed. In $\bar{p}p$ annihilation there is evidence for an isovector $2^{++}$ resonance with a mass of 1660 MeV and a width of 280 MeV [9], also reported in $\gamma\gamma$ collisions [10]. The work presented here clarifies some of these issues.

## 2 Data Reconstruction and Selection

The Crystal Barrel detector, described elsewhere [11], consisted of a liquid hydrogen target with a length of 44 mm surrounded by a silicon vertex detector. Its detection efficiency for charged particles exceeded 99 %. Tracking information and identification of charged particles was given by the cylindrical jet drift chamber. The coverage was 95 % (64 %) of the full solid angle for the inner (outer) layers. Both devices were used to veto charged particles in the present analysis. They were surrounded by a barrel of CsI(Tl) crystals consisting of 1380 modules arranged in a vertex-pointing geometry over the range of polar angles $\theta$ from 12° to 168° and with full azimuthal coverage. The energy resolution for photons was given by $\sigma(E)/E = 2.8\%\ (E[\mathrm{GeV}])^{-1/4}$. The angular resolution was energy and $\theta$ dependent, typically 25 mrad. The whole assembly was located in a solenoid magnet providing a homogeneous field of 1.5 T, parallel to the incident antiproton beam.

The present analysis is based on 17.9 million events which were taken with the all-neutral trigger during the last data taking of Crystal Barrel at LEAR (CERN) in October 1996. The data selection only considered complete reconstructed events with exactly six clusters and no charged tracks. To improve the data quality, clusters with an energy of less than 13 MeV in the central crystal were rejected in order to remove spurious photons due to shower fluctuations. The energy of the central crystal in a cluster relative to the sum of all neighbouring crystals had to be less than 0.96 in order to reject clusters produced by secondary neutrons.

Figure 1 shows a two-dimensional scatter plot of the $2\gamma$ invariant mass for kinematically fitted $\pi^0 4\gamma$ events (confidence level CL > 1 %). Clear signals for $\pi^0\pi^0\pi^0$, $\pi^0\pi^0\eta$ and $\pi^0\eta\eta$ are observed.

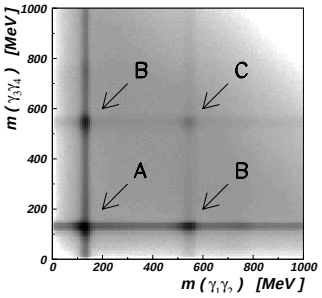


**Fig. 1.** Invariant mass $m(\gamma_1\gamma_2)$ versus $m(\gamma_3\gamma_4)$ for kinematically fitted $\overline{p}p \to \pi^0\gamma_1\gamma_2\gamma_3\gamma_4$ events (6 entries per event, logarithmic scale). One observes $\pi^0\pi^0\pi^0$ (A), $\pi^0\pi^0\eta$ (B) and $\pi^0\eta\eta$ (C) events.

In contrast to annihilations at rest, where the annihilation vertex is given within a few 100 microns by the momentum of the antiproton beam, for measurements in flight the annihilation vertex of purely neutral events cannot be observed. It must therefore be treated as a free parameter. The software library of Crystal Barrel provides a standard package for kinematic fitting, but the fitting procedure is not adequate in the present case due to strong correlations between the measured quantities. For this reason a completely new kinematic fitting program for 6 photon final states in flight was written. The program treats the coordinate of the annihilation vertex along the beam as a free parameter. Due to the small transverse size of the LEAR beam it was assumed that the annihilation vertex lies on the detector axis. The pull distributions are gaussian-like, as expected (Figure 2 left). The fits to the final states $\pi^0\pi^0\pi^0$, $\pi^0\pi^0\eta$ and $\pi^0\eta\eta$ were therefore 6 C fits.

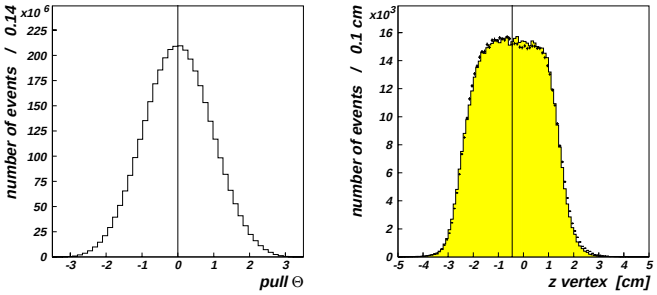


**Fig. 2.** Left: pull of $\theta$ for the selected $\pi^0\pi^0\pi^0$ events with the new fitting procedure. Right: z-vertex distribution for $\pi^0\pi^0\pi^0$ data (error bars) and Monte Carlo events (shaded histogram). The line gives the center of the distribution at -4.5 mm.

This new kinematic fit was then applied to the preselected 6 cluster events. A fit with a gaussian and a straight line to the $\eta$ peak in the $\gamma\gamma$ invariant mass distribution of events fulfilling the hypothesis $\overline{p}p \to \pi^0\pi^0\gamma\gamma$ gave

$$m_\eta = (547.26 \pm 0.04_{stat} \pm 0.65_{sys})\ \mathrm{MeV} \qquad (1)$$

and a width of 17 MeV compatible with our experimental resolution. The systematic errors were mainly due to un-

certanties in the calibration of the electromagnetic calorimeter. The mass is in excellent agreement with the PDG value [2].

Events were then accepted if one of the final states ($\pi^0\pi^0\pi^0$, $\pi^0\pi^0\eta$, $\pi^0\eta\eta$) had a confidence level of more than 10 %. The center of the target was found to be displaced by 4.5 mm with respect to the detector center (Figure 2). This displacement had to be taken into account for the final energy calibration of the crystals from $\pi^0 \to \gamma\gamma$ decays. In order to remove remaining events annihilating in the two veto counters behind the target, the fitted z-coordinate of the annihilation vertex was required to lie inside the target. The data selection presented here is therefore at variance with the one reported in ref. [12] which used a preliminary calibration assuming a vertex at the center of the detector.

In order to reduce the feedthrough between the different final states the $\pi^0\eta\eta$ data set required anti-cuts on $\pi^0\pi^0\pi^0$ (CL $< 10^{-5}$) and $\pi^0\pi^0\eta$ (CL $< 10^{-4}$) which reduced the contribution from these two channels to less than 0.7 %. The reaction $\overline{p}p \to \omega\omega$ with $\omega \to \pi^0\gamma$ and the $7\gamma$ channels $\omega\pi^0\pi^0$ and $\omega\eta\pi^0$ with a missing photon are the dominating background channels for $\pi^0\eta\eta$. Feedthrough from $\omega\omega$ could be reduced by fitting the $\omega\omega$ hypothesis and applying an anti-cut at the 1 % confidence level. The remaining $\omega\omega$ background could be neglected compared to $\omega\pi^0\pi^0$. Feedthrough from $\pi^0\omega$ and $\pi^0\eta$ was negligible compared to $\omega\pi^0\pi^0$. However, Monte Carlo simulation showed that $\eta\omega$ events misidentified as $\pi^0\eta\eta$ have preferably an invariant $\eta\eta$ mass of more than 1600 MeV. Therefore a kinematic fit on $\eta\omega$ (with a seventh undetected photon) was performed and an anti-cut at the 1 % confidence level applied. This led to 18′419 $\pi^0\eta\eta$ events with a detection and reconstruction efficiency of 26.5 %.

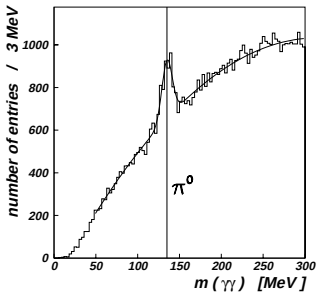


**Fig. 3.** Invariant $\gamma\gamma$ mass distribution for $\pi^0\eta\eta$ data events choosing those $\gamma\gamma$ combinations that were not selected by the best fit (12 entries per event). The line is at 135 MeV/$c^2$.

To avoid an excessive loss of good events, anti-cuts against $\omega\pi^0\pi^0$ and $\omega\eta\pi^0$ were not applied. Figure 3 shows the invariant $\gamma\gamma$ mass distribution for the selected 18′419 $\pi^0\eta\eta$ events, choosing those $\gamma\gamma$ combinations that were *not* selected by the kinematic fit as coming from $\pi^0\eta\eta$. There is a clear peak at the $\pi^0$ mass. This peak does not stem from $\pi^0\eta\eta$ events as shown by a Monte Carlo simulation of $\pi^0\eta\eta$ events. However, the simulated $\omega\pi^0\pi^0$ and $\omega\eta\pi^0$ events passing the selection criteria for $\pi^0\eta\eta$ produce a prominent $\pi^0$ peak. Therefore most events in the $\pi^0$ peak of Figure 3 are $\omega\pi^0\pi^0$ and to a lesser extent $\omega\eta\pi^0$ background events.

The absolute number of background events in the $\pi^0\eta\eta$ data set cannot be calculated directly as branching fractions for $\omega\pi^0\pi^0$ (and $\omega\eta\pi^0$) are not available for $\overline{p}p$ annihilation at 900 MeV/$c$. In order to get the absolute number of background events, the invariant $\gamma\gamma$ mass distribution of Figure 3 was simulated by adding the corresponding plots for Monte Carlo $\pi^0\eta\eta$, $\omega\pi^0\pi^0$ and $\omega\eta\pi^0$ events, assuming phase space distribution: the invariant mass distributions of $\omega\pi^0\pi^0$ and $\omega\eta\pi^0$ were added taking into account the feedthrough probabilities (of 3.1 : 1.0) and the branching ratios at rest in order to create the $\gamma\gamma$ distribution of the background events. Since the cross section for $\pi^0\eta\eta$ is not known, the number of these background events was scaled by a factor until the best match between data histogram and simulated histogram was achieved. We obtained $(2'338 \pm 145)$ background events or $(12.7 \pm 0.8)$ % background in the $\pi^0\eta\eta$ data set. The background was then simulated assuming phase space distribution. The simulated background events with the scaling factor were included in the subsequent partial wave analysis. We have verified that a non uniform population of e.g. the $\omega\pi^0\pi^0$ Dalitz plot, as was observed at rest [13], leads to the same results. The calculated number of true $\pi^0\eta\eta$ data events was $(16'081 \pm 199)$.

The $\pi^0\pi^0\eta$ data set required an anti-cut on $\pi^0\pi^0\pi^0$ only (CL $< 10^{-3}$) to reduce the background from that channel to less than 0.5 % while $\pi^0\eta\eta$ events misidentified as $\pi^0\pi^0\eta$ were negligible. Feedthrough from $\overline{p}p \to \omega\omega$ could be reduced to a negligible level by an anti-cut at 1 % confidence level. After these selection cuts 161′158 $\pi^0\pi^0\eta$ data events remained. The total efficiency for $\pi^0\pi^0\eta$ was 26.6 %.

For the determination of the dominant $\omega\pi^0\pi^0$ background in the $\pi^0\pi^0\eta$ data set the same procedure as for the $\pi^0\eta\eta$ data was used. We obtained $(4'272 \pm 209)$ events or $(2.7 \pm 0.2)$ % background events in the $\pi^0\pi^0\eta$ data set. These $\omega\pi^0\pi^0$ background events were included in the subsequent partial wave analysis. The calculated number of true $\pi^0\pi^0\eta$ data events was $(156'886 \pm 453)$.

In the $\pi^0\pi^0\pi^0$ data set the misidentified $\pi^0\pi^0\eta$ and $\pi^0\eta\eta$ events and the background from various other channels ($(0.4 \pm 0.1)$%) were negligible. This led to 600′962 $\pi^0\pi^0\pi^0$ events with a selection efficiency of 26.9 %.

The ratio of cross sections for $\pi^0\pi^0\pi^0$, $\pi^0\pi^0\eta$ and $\pi^0\eta\eta$ in $\overline{p}p$ annihilation at 900 MeV/$c$ (corrected for reconstruction efficiencies and for the unobserved $\pi^0$ and $\eta$ decay modes) are:

$$\pi^0\pi^0\pi^0 : \pi^0\pi^0\eta : \pi^0\eta\eta = 1 \ : \ 0.66 \pm 0.02 \ : \ 0.17 \pm 0.01 \ .$$

These numbers were corrected for reconstruction efficiencies and for the unobserved $\pi^0$ and $\eta$ decay modes. The corresponding branching ratios at rest scales as $1 : 1.08 \pm 0.26 : 0.32 \pm 0.08$ [14–16].

The symmetrised $\pi^0\pi^0\pi^0$ Dalitz plot is shown in the upper left side of Figure 4. No acceptance correction was applied. Three structures are observed: a) a prominent band around 1300 MeV (arrow A) which is identified with the $f_2(1270)$ decaying into $\pi^0\pi^0$; b) around 1500 MeV a

relatively uniformly populated band (arrow B) appears which is produced by the $f_0(1500)$ and/or $f_2(1565)$; c) arrow C points to a faint dip in the 1500 MeV band around 1000 MeV which corresponds to the $f_0(980)$ interfering destructively with the structure at 1500 MeV.

Figure 4 upper right shows the Dalitz plot for $\pi^0\pi^0\eta$. No acceptance correction was applied. Its features are as follows: a) the $\pi^0\pi^0$ system shows a strong enhancement (arrow A) around 1300 MeV corresponding to the $f_2(1270)$; b) at 1000 MeV (arrow B) a band is produced by the $f_0(980)$. In contrast to its production in $\pi^0\pi^0\pi^0$, it interferes constructively here; c) in $\pi^0\eta$ the prominent structure around 1300 MeV (arrow C) is the $a_2(1320)$; d) the flat bands around 1000 MeV in the $\pi^0\eta$ system (arrow D) are due to the $a_0(980)$ decaying into $\pi^0\eta$; e) the accumulation of events at small $\pi\pi$ masses (along the diagonal boundary) is due to interference between the two $a_2(1320)$ bands.

The symmetrised $\pi^0\eta\eta$ Dalitz plot is shown in Figure 4 lower left. The following structures are observed: a) a band around 1000 MeV (arrow A) in the $\pi^0\eta$ system which is due to the $a_0(980)$; b) the $a_2(1320)$ decaying into $\pi^0\eta$ (arrow B); c) in the $\eta\eta$ system only one structure around 1500 MeV is observed (arrow C), flat in the middle and slightly enhanced at the edges of the Dalitz plot, due to the $f_0(1500)$ and/or $f_2'(1525)$; d) around 1700 MeV, the region of the $f_0(1710)$, only the crossing of the two $a_0(980)$ bands can be observed (arrow D), no obvious signal being present.

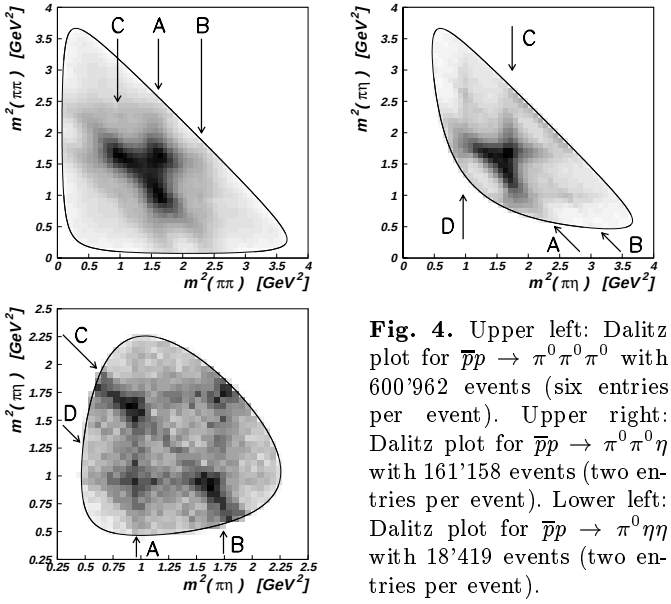


**Fig. 4.** Upper left: Dalitz plot for $\overline{p}p \to \pi^0\pi^0\pi^0$ with 600'962 events (six entries per event). Upper right: Dalitz plot for $\overline{p}p \to \pi^0\pi^0\eta$ with 161'158 events (two entries per event). Lower left: Dalitz plot for $\overline{p}p \to \pi^0\eta\eta$ with 18'419 events (two entries per event).

## 3 Analysis Method

The qualitative features described above were confirmed by a partial wave analysis. The data sets were analysed in the helicity formalism [17] in terms of the isobar model [18], in which the $\overline{p}p$ system is assumed to decay into the 3-body final states through a two-body intermediate state made of resonance and spectator meson. The transition amplitude for this process, where the $\overline{p}p$ system has given $J^{PC}$ and helicity $M$, was expressed as

$$A_M^{J^{PC}} = \sum_{\nu,\lambda} H_\nu^{J^{PC}} \cdot f_{\lambda,M}(\Omega,\Omega') \cdot F(m) \,, \qquad (2)$$

where the sum extended over all possible initial and final state helicities $\nu$ and $\lambda$, respectively. $H_\nu^{J^{PC}}$ describes the production process of the $\overline{p}p$ system. As the production angles are fixed by the free choice of the z-axis, this transition amplitude reduces to a complex constant $H_{\nu_1,\nu_2}^{J^{PC}}$ with $\nu_1,\nu_2 = \pm\frac{1}{2}$ the helicities of the proton and antiproton and $\nu = \nu_1 - \nu_2$ the total helicity of the $\overline{p}p$ system. Spin-singlet states have $H_{+-}^{J^{PC}} = H_{-+}^{J^{PC}} = 0$ as $S = 0$ and therefore the projection $M = \nu$ onto the beam axis vanishes. The relative angular momentum $L$ is perpendicular to the beam axis and does not contribute to the helicity. The spin-wavefunction for spin-triplet states is given by $\Psi = (H_{++}^{J^{PC}} + H_{--}^{J^{PC}})/\sqrt{2}$. Spin-triplet states with odd spin have $H_{++}^{J^{PC}} = -H_{--}^{J^{PC}}$ and therefore the $\nu = 0$ amplitude vanishes. The amplitude $f_{\lambda,M}(\Omega,\Omega')$ parametrises the angular dependence of the decay. For $\overline{p}p$ decaying into a pseudoscalar meson and a resonance (decaying in turn into two pseudoscalar mesons), it is given by

$$f_{\lambda_1,M}(\Omega,\Omega') = \mathcal{D}^J_{\lambda_1,M}(\theta,\phi) \cdot \mathcal{D}^s_{0,\lambda_1}(\theta',\phi') \cdot \sum_{l,s} \alpha_{l,s} \, \langle J\lambda_1 | ls0\lambda_1 \rangle \,, \qquad (3)$$

where $J$ and $M$ are the spin and the magnetic substates of the $\overline{p}p$ system, $s$ and $\lambda_1$ the spin and the helicity of the resonance, $l$ is the angular momentum between resonance and spectator meson, $\theta,\phi$ are the production angles of the resonance in the $\overline{p}p$ center of mass system and $\theta',\phi'$ are the decay angles of the resonance in its rest frame.

In eqn. (2) $F(m)$ is the dynamical function for which the P-vector approach [19][20] in the $K$-matrix formalism was used to describe resonances of the same quantum numbers within a partial wave. Following Aitchison [19] the dynamical function is then given by

$$F = (\mathbf{1} - iK\rho)^{-1} P \,, \qquad (4)$$

where the $K$-matrix is defined as a sum of poles with masses $m_\alpha$ describing all contributing resonances:

$$K_{ij} = \sum_\alpha \frac{g_{\alpha i} g_{\alpha j} D^l(q_i,q_\alpha) D^l(q_j,q_\alpha)}{m_\alpha^2 - m^2} + c_{ij} \,. \qquad (5)$$

The couplings $g_{\alpha i}$ are given by the partial widths $\widetilde{\Gamma}_{\alpha i}$:

$$g_{\alpha i} = \sqrt{\frac{m_\alpha \widetilde{\Gamma}_{\alpha i}}{\rho_i(m_\alpha)}} \,, \qquad (6)$$

where $\rho_i$ is the two-body phase space factor for the decay into a particular channel $i$. The $c_{ij}$ are real and symmetric

background constants. The $D^l(q_i, q_\alpha)$ are ratios of Blatt-Weisskopf centrifugal barrier factors [21] in terms of the break-up momentum $q_i$ in channel $i$ and the resonance break-up momentum $q_\alpha$ for the orbital angular momentum $l$.

The production vector $P$ has the same poles as the $K$-matrix but the couplings $g_{\alpha i}$ to the initial channels are replaced by couplings $\beta^0_\alpha$ to the annihilation vertex of the $\overline{p}p$ system:

$$P_i = \sum_\alpha \frac{\beta^0_\alpha \, g_{\alpha i} D^l(q_i, q_\alpha)}{m^2_\alpha - m^2} \tag{7}$$

with the normalisation

$$\beta^0_\alpha = \beta_\alpha \sqrt{\sum_i g^2_{\alpha i}} \ . \tag{8}$$

In the case of the $(\pi\pi)_S-$wave $K$ was multiplied by a factor $(m^2 - 2m^2_\pi)/m^2$ to characterise the behaviour near the $\pi\pi$ threshold.

Spin-singlet and spin-triplet partial waves are added incoherently and there is no interference between partial waves with different $\overline{p}p$ helicities $M$. For a given set of $S$ and $M$ all possible transition amplitudes are summed coherently. The total transition probability $w$ for each event is then the incoherent sum over spin-singlet and spin-triplet amplitudes with different $M$:

$$\begin{aligned} w = &\left|\sum A^{S=0}_{M=0}\right|^2 + \left|\sum A^{S=1}_{M=-1}\right|^2 \\ &+ \left|\sum A^{S=1}_{M=0}\right|^2 + \left|\sum A^{S=1}_{M=+1}\right|^2 \ . \end{aligned} \tag{9}$$

While annihilation at rest proceeds mainly from $S-$states [22], with increasing energies more initial states contribute. A previous Crystal Barrel analysis [23] indicated that $\overline{p}p$ initial states up to $J = 3$ should be sufficient to describe the data at 900 MeV/$c$ satisfactorily. In the subsequent partial wave analyses the $J = 4$ contributions to the data sets were less than 5 % and contributions from $J \geq 4$ were therefore neglected.

The parameters to be determined by the fits were masses and widths of the involved resonances, the production parameters $\alpha_{l,s}$ for these resonances and the $\overline{p}p$ amplitudes $H^{J^{PC}}_{\nu_1,\nu_2}$. The $\overline{p}p$ amplitudes and their symmetry properties are shown in Table 1. When only $\overline{p}p$ initial states up to $J = 3$ are considered, 6 $\overline{p}p$ amplitudes and for every scalar (tensor) resonance 4 (11) production parameters $\alpha_{l,s}$ had to be determined. Out of the 12 real parameters for the $\overline{p}p$ amplitudes $H^{J^{PC}}_{\nu_1,\nu_2}$ eight are arbitrary and were fixed. Additional 5 phases (one for every initial state) for the production amplitudes are arbitrary and were fixed to 0.

The $(\pi\pi)_S-$wave was parametrised as a $(3 \times 3)$ $K$-matrix with four poles. The four poles correspond to the $f_0(600)$, $f_0(980)$, $f_0(1370)$ and $f_0(1500)$. The pole parameters including the channels $\pi\pi$, $K\bar{K}$ and $\eta\eta$ were taken from the analysis of the $\pi^0\pi^0\pi^0$, $\pi^0\pi^0\eta$ and $\pi^0\eta\eta$ final states at rest [1]. When testing for the $f_0(1710)$ a fifth pole was not introduced into the $K$-matrix of the $(\pi\pi)_S-$wave because that would have required refitting the $K$-matrix parameters of the four other poles. This was not possible with the current data sets alone. In fact, the $K$-matrix parameters were well determined in the coupled channel analysis at rest [1] where the $(\pi\pi)_S-$wave was the dominant contribution and where more constraints (well determined $\overline{p}p$ initial state) apply than for in flight analyses. Therefore, the $K$-matrix parameters were adopted unmodified. However, as the reported $f_0(1710)$ is quite narrow, the approximation of a $K$-matrix and a Breit-Wigner amplitude for the total $(\pi\pi)_S-$intensity is valid.

| $\overline{p}p$ initial state | | $\nu = 0$ | $\nu = \pm 1$ |
|---|---|---|---|
| $^1S_0$ | $(0^{-+})$ | $H_{++} = -H_{--}$ | 0 |
| $^3P_1$ | $(1^{++})$ | 0 | $H_{+-} = -H_{-+}$ |
| $^3P_2, ^3F_2$ | $(2^{++})$ | $H_{++} = H_{--}$ | $H_{+-} = H_{-+}$ |
| $^1D_2$ | $(2^{-+})$ | $H_{++} = -H_{--}$ | 0 |
| $^3F_3$ | $(3^{++})$ | 0 | $H_{+-} = -H_{-+}$ |

**Table 1.** Symmetry properties of the production amplitudes $H^{J^{PC}}_{\nu_1,\nu_2}$ for $\overline{p}p$ initial states up to $J = 3$. $\nu$ is the total helicity of the $\overline{p}p$ system.

The $(\pi\eta)_S-$wave was parametrised as $(2 \times 2)$ $K$-matrix with couplings to $\pi\eta$ and $K\bar{K}$ and poles for the $a_0(980)$ and $a_0(1450)$ [1]. For the other resonances the masses and widths were taken from the tables of the particle data group (PDG) [2].

We maximised the extended likelihood function $\mathcal{L}$:

$$\mathcal{L} = N! \prod_{i=1}^{N} \frac{w_{data}}{\int w_{MC}} \cdot \exp\left(-\frac{(N - \int w_{MC})^2}{2\,N}\right), \tag{10}$$

where $N$ is the number of data events and $w_{data}$, $w_{MC}$ eqn. (9) evaluated for data and Monte Carlo events, respectively. The feedthrough of background in the $\pi^0\pi^0\eta$ and $\pi^0\eta\eta$ data sets was taken into account by rescaling the likelihood function with the likelihood for the background events [24] $\mathcal{L}' = \mathcal{L}_{data}/\mathcal{L}_{BG}$, where $\mathcal{L}_{data}$, $\mathcal{L}_{BG}$ are given by eqn. (10), evaluated for data and background events, respectively.

Calculation of the likelihood function $\mathcal{L}$ for the 600'962 $\pi^0\pi^0\pi^0$ events is extremely consuming in terms of computing time. An efficient way to reduce the number of calculations while minimising the memory requirements is the binning of the functions $F$ and $\mathcal{D}$ in eqns. (2) and (3). Every event is assigned a set of indices corresponding to $\theta, \phi, \theta', \phi'$ and the invariant masses for the three possible two-body invariant mass systems [25]. $\mathcal{D}^J_{\lambda_1,M}(\theta, \phi)$, $\mathcal{D}^s_{0,\lambda_1}(\theta', \phi')$ and $F$ were then evaluated at the center of each bin for every occurring combination of $J$, $\lambda_1$, $M$ and $s$. For the present analysis the binning was chosen to be 2 degrees for all angles (90 bins in $\theta, \theta'$ and 180 bins in $\phi, \phi'$) and 1000 bins for invariant masses. This reduced the number of calculations for the whole $\pi^0\pi^0\pi^0$ data set by a factor of $\approx 10^5$.

The fitting program was written in FORTRAN based on the MINUIT [26] program package and required for 100'000 events 60 - 120 megabytes of main memory, depending on the number of involved resonances. In order to fit the full $\pi^0\pi^0\pi^0$ and $\pi^0\pi^0\eta$ data sets the program was ported to a NEC SX-5 supercomputer architecture [27]. The tuned program achieved on a single SX-5 processor an average of 2.1 gigaflops.

## 4 Fit Results of $\overline{p}p \to \pi^0\pi^0\pi^0$

The first description of $\pi^0\pi^0\pi^0$ included the $(\pi\pi)_S-$ wave and the $f_2(1270)$. The fit with 53 free parameters converged to a $S = -\ln\mathcal{L}$ of $-420'526$. At high $\pi^0\pi^0$ invariant masses the fit did not describe satisfactorily the data and the contribution of the $f_0(980)$ was overestimated. Extending this fit with the $f_0(1710)$ which was parametrised as Breit-Wigner amplitude with values of $m = 1715$ MeV and $\Gamma = 125$ MeV for mass and width [2] resulted in $S = -422'432$. The $f_0(1710)$ with fixed mass and width contributed $(2.0\pm1.0)$ % to the $\pi^0\pi^0\pi^0$ data set. With free mass and width of the $f_0(1710)$ the fit converged to $S = -427'659$. However, the resulting parameters for this additional scalar resonance were $m = 1338$ MeV and $\Gamma = 856$ MeV, indicating that the fit tried to compensate for missing information.

The next fit extended the first hypothesis with a second pole in the $(\pi\pi)_D-$wave to test for a spin 2 meson. The $K$-matrix parameters were chosen so that the $T$-matrix resonance parameters of the $f_2(1270)$ agreed with the PDG values [2]. With free $K$-matrix pole parameters for a second pole in the $(\pi\pi)_D-$wave $S$ decreased to $-433'113$. The change in $S$ per parameter was $12'587/24 = 524$, 2.5 times that of the previous fit for the $f_0(1710)$. The fit clearly preferred as additional resonance to the minimum hypothesis a high-mass tensor state. The $T$-matrix pole parameters for the high-mass tensor were $m = 1876$ MeV and $\Gamma = 408$ MeV. This resonance contributed 22 % to the $\pi^0\pi^0\pi^0$ data set. The description of the data set was already quite reasonable.

This fit was then extended with a $f_0(1710)$, again parametrised as Breit-Wigner amplitude. The fit converged with a contribution of the $f_0(1710)$ of $(0.8\pm0.5)$ %. The improvement of 667 in $S$ was not significant. The fit with free $f_0(1710)$ parameters led to $m = 1275$ MeV and $\Gamma = 770$ MeV and was therefore rejected.

The best fit to the $\pi^0\pi^0\pi^0$ data was obtained by parametrising the $(\pi\pi)_D-$wave as $K$-matrix with three poles. With the $f_2(1270)$ pole fixed the fit had 101 free parameters to determine. The fit converged to $S = -435'491$, a significant improvement of $2'378$ units. The resulting $K$-matrix parameters for the $(\pi\pi)_D-$wave are listed in Table 2. The errors on mass and width include the variability for various fits. The resonance parameters of the second pole agree well with the PDG values for the $f_2(1565)$, $m = (1544\pm17)$ MeV/$c^2$ and $\Gamma = (131\pm14)$ MeV/$c^2$ [2]. The second pole is therefore identified with the $f_2(1565)$. The resonance at 1929 MeV, which we call $f_2(1870)$, is new.

Figure 5 shows the $\pi^0\pi^0$ mass projection and the residual $\chi^2$ over the $\pi^0\pi^0\pi^0$ Dalitz plot. We emphasize that the description of the $\pi\pi$ S-wave was taken from our results at rest, e.g. the $f_0(980)$ was not refitted independently of the $(\pi\pi)_S$ -wave. This explains the small residual $f_0(980)$ signal in fig. 5 right. The combined contribution of $f_0(600)$, $f_0(980)$ and $f_0(1370)$ which cannot be disentangled due to interferences was $(17\pm3)$ %. The $f_0(1500)$ contributed $(10\pm2)$ %. The contributions were $(46\pm5)$ %, $(15\pm3)$ % and $(12\pm3)$ % for the $f_2(1270)$, $f_2(1565)$ and $f_2(1870)$, respectively.

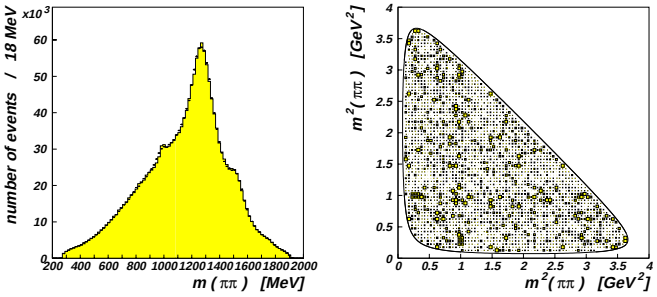


**Fig. 5.** Left: Invariant mass $m(\pi^0\pi^0)$ (three entries per event) for the best fit for $\pi^0\pi^0\pi^0$. The dots show the data, the shaded histogram the fit. Right: Distribution of the residual $\chi^2$. Bins at the edge of the Dalitz plot are ignored. The largest squares correspond to a $\chi^2$ contribution of at least 9.

This best fit was again checked against an $f_0(1710)$. It converged with $S = -436'077$. However, the $K$-matrix poles of the $(\pi\pi)_D-$wave had to be fixed to the values of the best fit in order to get proper convergence. Again, the improvement of $S$ was not significant. In this fit the $f_0(1710)$ contributed with $(0.8\pm0.5)$ % to the $\pi^0\pi^0\pi^0$ data set. When the $f_0(1710)$ mass and width and the pole parameters of the two upper poles of the $(\pi\pi)_D-$wave were freely fitted, the fit converged to $S = -437'463$. The $f_0(1710)$ contributed 3.9 % and the parameters of the $f_0(1710)$ were $m = 1858$ MeV and $\Gamma = 153$ MeV. However, the high mass $(\pi\pi)_D-$wave pole was pushed far out of phase space to $m = 2360$ MeV and $\Gamma = 420$ MeV and this fit was therefore rejected.

As none of the fits including an $f_0(1710)$ had stable solutions, the conclusion was drawn that the $f_0(1710)$ is not present in the $\pi^0\pi^0\pi^0$ data set in flight at 900 MeV/$c$. The upper limit for the contribution of the $f_0(1710)$ ($m = 1715$ MeV, $\Gamma = 125$ MeV [2]) to $\pi^0\pi^0\pi^0$ is 1.5 % at 90 % confidence level.

## 5 Fit Results of $\overline{p}p \to \pi^0\pi^0\eta$

The first description of $\pi^0\pi^0\eta$ consisted of the $(\pi\pi)_S-$wave, the $f_2(1270)$, the $a_0(980)$ and $a_0(1450)$ in the $(\pi\eta)_S-$wave and the $a_2(1320)$. This minimum hypothesis included a total of 6 scalar and 2 tensor resonances, resulting in 91 parameters to be fitted. The minimum fit converged with

| $\pi^0\pi^0\pi^0$ | $m_\alpha$ [ MeV ] | $\widetilde{\Gamma}_{\alpha,\pi\pi}$ [ MeV ] | $T$-matrix poles [ MeV ] | | $\pi^0\eta\eta$ | $m_\alpha$ [ MeV ] | $\widetilde{\Gamma}_{\alpha,\eta\eta}$ [ MeV ] | $T$-matrix poles [ MeV ] | |
|---|---|---|---|---|---|---|---|---|---|
| $f_2(1270)$ | 1230 | 200 | 1274 | 187 | $f_2'(1525)$ | $1504 \pm 10$ | $76 \pm 10$ | $1516 \pm 10$ | $74 \pm 11$ |
| $f_2(1565)$ | $1545 \pm 10$ | $128 \pm 20$ | $1554 \pm 12$ | $147 \pm 27$ | $f_2(1870)$ | $1855\ ^{+50}_{-10}$ | $343 \pm 40$ | $1820\ ^{+57}_{-10}$ | $358 \pm 42$ |
| $f_2(1870)$ | $1929 \pm 25$ | $309 \pm 50$ | $1877 \pm 30$ | $318 \pm 55$ | | | | | |

**Table 2.** $K$-matrix parameters and the corresponding $T$-matrix poles of the $(\pi\pi)_D-$wave for $\pi^0\pi^0\pi^0$ (left) and of the $(\eta\eta)_D-$wave for $\pi^0\eta\eta$ (right). For $\pi^0\pi^0\pi^0$ the $f_2(1270)$ parameters were fixed.

$S = -113'366$. The agreement between data and fit was good, the $f_0(980)$ being slightly underestimated.

In the Crystal Barrel analysis of $\pi^0\pi^0\eta$ at rest [15] there was evidence for a resonance between 1600 - 1700 MeV in the $(\pi\eta)_D-$wave. The Crystal Barrel analysis of $\pi^0\eta\eta$ in flight at 1940 MeV/$c$ [9] also reported an isovector state $a_2(1660)$ decaying into $\pi^0\eta$ with $m = (1660 \pm 40)$ MeV and $\Gamma = (280 \pm 70)$ MeV. Hence the $a_2(1660)$ was introduced into the $(1 \times 1)$ $K$-matrix of the $(\pi\eta)_D-$wave as a second pole. The $K$-matrix pole parameters of the $a_2(1320)$ were re-adjusted so that the $T$-matrix pole agreed with PDG values. The fit converged to $S = -115'889$ which is a significant improvement for 24 additional parameters. The fitted projections together with the data and the residual $\chi^2$ are shown in Figure 6. The $f_0(980)$ was now well described. The $T$-matrix parameters (Table 3) for the $a_2(1660)$ are in good agreement with the previous Crystal Barrel analysis [9]. The $a_2(1660)$ contributes with $(7 \pm 2)$ % to the data. The contributions of all resonances are compiled in Table 4. The contributing amplitudes were integrated over phase space and then normalised to the total sum to obtain the relative contributions. No errors are given for the contributions of the resonances from the individual initial states as they can vary considerably. However, the total contributions of the resonances are stable within the given errors.

A further fit allowed free variation of the $K$-matrix parameters of the $a_0(1450)$, resulting in a total of 118 free parameters. The $T$-matrix pole position was then $m = (1296 \pm 10)$ MeV, $\Gamma = (81 \pm 21)$ MeV. These parameters agree well with the ones found in the analysis of $K^\pm K_S \pi^\mp$ by the Obelix Collaboration of $m = (1.29 \pm 0.01)$ GeV and $\Gamma = (0.080 \pm 0.005)$ GeV [4]. The mass and width of the $a_2(1660)$ did not change significantly (Table 3). $S$ changed by 1976 to $-117'865$ with only three more parameters. The significance of this result is discussed in section 8.6 below. The contributions of the other resonances changed within errors, the contribution of the $a_2(1660)$ increased slightly to $(10 \pm 2)$ % as some of the intensity formerly attributed to the $a_0(1450)$ was then described by the $a_2(1660)$. The $a_0(1300)$ contributed $(7 \pm 1)$ % to $\pi^0\pi^0\eta$.

We tried to combine the $a_0(1300)$ and the $a_0(1450)$ in the $(\pi\eta)_S-$wave by introducing a third pole into the $(2 \times 2)$ $K$-matrix. These fits gave neither a significant improvement nor stable solutions.

The contribution to $\pi^0\pi^0\eta$ of exotic $1^{-+}$ resonances decaying into $\pi^0\eta$ is completely negligible. The $\pi_1(1400)$ and

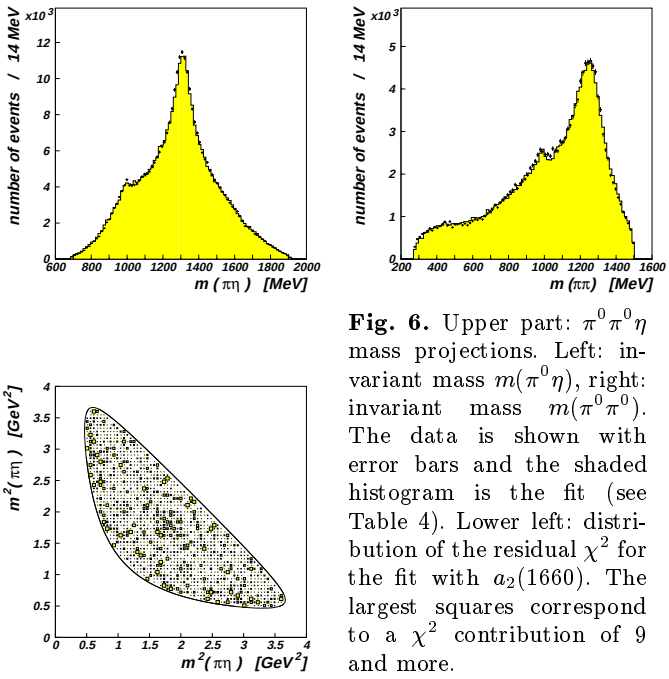


**Fig. 6.** Upper part: $\pi^0\pi^0\eta$ mass projections. Left: invariant mass $m(\pi^0\eta)$, right: invariant mass $m(\pi^0\pi^0)$. The data is shown with error bars and the shaded histogram is the fit (see Table 4). Lower left: distribution of the residual $\chi^2$ for the fit with $a_2(1660)$. The largest squares correspond to a $\chi^2$ contribution of 9 and more.

$\pi_1(1600)$ were parametrised as relativistic Breit-Wigner amplitudes with PDG values [2] for mass and width. The log-likelihood changed insignificantly and the contributions were negligible.

## 6 Fit Results of $\bar{p}p \to \pi^0\eta\eta$

The first description of $\pi^0\eta\eta$ included the $a_0(980)$ and $a_0(1450)$ in the $(\pi\eta)_S-$wave (fixed values from ref. [1]) and the $a_2(1320)$ in the $(\pi\eta)_D-$wave. For the $(\eta\eta)_S-$wave the $(3 \times 3)$ $K$-matrix with four poles from ref. [1] was used where only the two upper poles, the $f_0(1370)$ and $f_0(1500)$, were allowed to be produced. Therefore, the first description included 4 scalar and one tensor resonance, hence a total of 53 parameters to be fitted. The minimum fit converged to $S = -7'387$. The fitted projection together with the data is shown in the upper left part of Figure 7 for the $\eta\eta$ invariant mass. Significant differences between fit and data were observed in the region around $\eta\eta$ invariant masses of $1500-1550$ MeV and $1650-1800$ MeV. The $\pi^0\eta$ invariant mass (not shown) was already well described.

This basic fit was extended by adding a scalar or tensor resonance to test for the $f_J(1710)$, both parametrised

| | $m_\alpha$ [ MeV ] | $\widetilde{\Gamma}_{\alpha,\pi\eta}$ [ MeV ] | $T$-matrix poles [ MeV ] | | | $m_\alpha$ [ MeV ] | $\widetilde{\Gamma}_{\alpha,\pi\eta}$ [ MeV ] | $T$-matrix poles [ MeV ] | |
|---|---|---|---|---|---|---|---|---|---|
| $a_2(1320)$ | 1307 | 105 | 1317 | 108 | | $a_2(1320)$ | 1307 | 105 | 1318 | 107 |
| $a_2(1660)$ | $1726 \pm 40$ | $229 \pm 60$ | $1706 \pm 42$ | $235 \pm 65$ | | $a_2(1660)$ | $1723 \pm 40$ | $259 \pm 50$ | $1698 \pm 44$ | $265 \pm 55$ |

**Table 3.** $K$-matrix parameters and corresponding $T$-matrix poles of the $(\pi\eta)_D-$wave for the fits with the $a_0(1450)$ (left) and the $a_0(1300)$ (right). The $a_2(1320)$ parameters were fixed.

| $\overline{p}p$ partial wave | $0^{-+}$ | $1^{++}$ | $2^{-+}$ | $2^{++}$ | $3^{++}$ | $\sum$ |
|---|---|---|---|---|---|---|
| $(\pi\pi)_S\ \eta$ | 1 | 8 | 6 | | 1 | $15 \pm 3$ |
| $f_0(1500)\ \eta$ | 1 | 1 | 1 | | 0 | $3 \pm 1$ |
| $f_2(1270)\ \eta$ | 1 | 4 | 14 | 7 | 5 | $31 \pm 3$ |
| $a_0(980)\ \pi^0$ | 2 | 1 | 1 | | 2 | $6 \pm 1$ |
| $a_0(1450)\ \pi^0$ | 2 | 2 | 0 | | 1 | $5 \pm 1$ |
| $a_2(1320)\ \pi^0$ | 2 | 20 | 6 | 5 | 1 | $33 \pm 3$ |
| $a_2(1660)\ \pi^0$ | 0 | 1 | 2 | 3 | 1 | $7 \pm 2$ |
| $\sum$ | 11 | 31 | 27 | 17 | 14 | 100 |

**Table 4.** Contributions in % to $\pi^0\pi^0\eta$. $(\pi\pi)_S$ includes contributions of $f_0(600)$, $f_0(980)$ and $f_0(1370)$, which cannot be disentangled due to interferences.

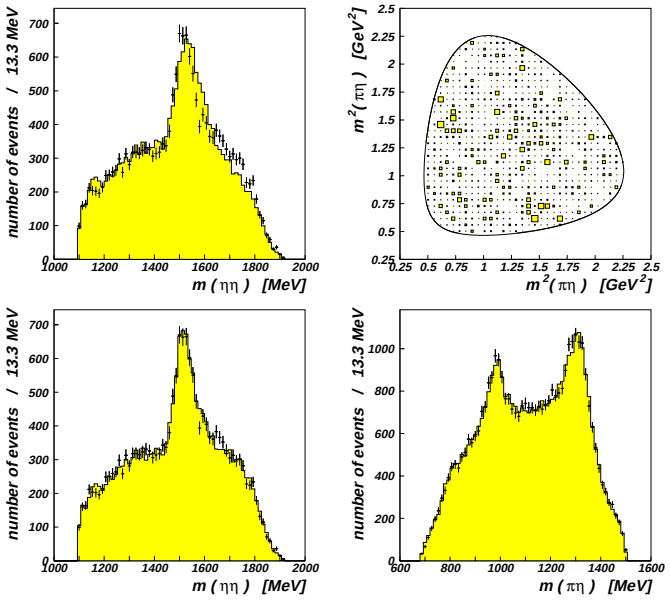


**Fig. 7.** Upper left: first description of $\pi^0\eta\eta$: invariant mass $m(\eta\eta)$. Upper right: best fit of $\pi^0\eta\eta$: Distribution of the residual $\chi^2$. The largest squares correspond to a $\chi^2$ contribution of 9 and more. Lower left: best fit of $\pi^0\eta\eta$: invariant mass $m(\eta\eta)$. Lower right: invariant mass $m(\pi^0\eta)$ (two entries per event).

as Breit-Wigner functions with fixed values of $m = 1715$ MeV and $\Gamma = 125$ MeV [2]. The fit with a $f_0(1710)$ converged with $S = -7'692$ where the $f_0(1710)$ contributed with $(8 \pm 1)$ % to the $\pi^0\eta\eta$ data set. The parameters of this scalar resonance became $m = 1648$ MeV and $\Gamma = 249$ MeV when fitted freely and $S$ improved to $-7'825$. The high-mass region in the $\eta\eta$ invariant mass was quite well described but the peak around 1500 MeV still missed intensity. However, this scalar state contributed 22 % to the data set and produced strong interferences with the $a_0(980)$ and $f_0(1500)$.

The fit with a tensor $f_J(1710)$ converged with $S = -7'791$. When the mass and width of this tensor resonance were fitted (7 parameters to determine), the fit converged to $m = 1905$ MeV and $\Gamma = 387$ MeV with $S = -7'990$ where the parameters of this tensor state agree quite well with that of the high-mass tensor required in the analysis of $\pi^0\pi^0\pi^0$ of $m = (1877 \pm 30)$ MeV and $\Gamma = (318 \pm 55)$ MeV. This high mass tensor had a contribution of 23 % to the $\pi^0\eta\eta$ data set. Again, the high-mass region was well described but the peak around 1500 MeV missed intensity. This tensor state produced only minor interference effects with the $a_0(980)$ and $f_0(1500)$.

To describe the peak around 1500 MeV in the $\eta\eta$ invariant mass, the tensor resonance $f_2'(1525)$ was then introduced into both previous fits. The $f_2'(1525)$ was parametrised as a Breit-Wigner function in the fit with the $f_0(1710)$. The freely fitted parameters of the $f_2'(1525)$ were then $m = 1502$ MeV and $\Gamma = 78$ MeV with $S = -8'245$. The mass is slightly too low but the width is well within PDG errors. The scalar resonance had a mass of 1709 MeV and width $\Gamma = 349$ MeV. However, the stability of the fit was poor.

For the fit with the tensor $f_J(1710)$ the $(\eta\eta)_D-$wave was parametrised as a $(1 \times 1)$ $K$-matrix with two poles and couplings to $\eta\eta$ in order to include the $f_2'(1525)$. When the $K$-matrix parameters of the $(\eta\eta)_D-$wave were fitted 101 parameters had to be determined. This fit converged to a $S$ of $-8'393$. The resulting $T$-matrix poles of the $(\eta\eta)_D-$wave (Table 2) were $m = (1516 \pm 10)$ MeV and $\Gamma = (74 \pm 11)$ MeV and $m = (1820\ ^{+}_{-}\ ^{57}_{10})$ MeV and $\Gamma = (358 \pm$

42) MeV. The parameters of the $f_2'(1525)$ agree well with the PDG values [2]. The mass and width of the $f_2(1870)$ agree with the ones found in the analysis of $\pi^0\pi^0\pi^0$. It is likely that these two states are identical. The consistency is described in the following section where both data sets were fitted simultaneously.

The change in log-likelihood per parameter from the basic fit was $858/34 = 25$ for the fit with a scalar and a tensor resonance and $1006/48 = 21$ for the fit with two isoscalar tensor resonances. However, reducing the number of parameters by neglecting initial states for the isoscalar tensor resonances with very small contributions gave a change of $988/40 = 25$ per parameter. The changes of the other fitted parameters were well within the errors. As both fits improved the log-likelihood per parameter the same, but the second one had a better pseudo-$\chi^2$ over the Dalitz plot and the parameters of this fit were very stable, the fit with the two isoscalar tensor resonances was considered to be the better fit.

Figure 7 upper right shows the pseudo-$\chi^2$ per bin for the best fit. The two projections of the $\eta\pi$ and $\eta\eta$ invariant masses are shown in the lower part of Figure 7. The data are very well described and there are no significant deviations. The $f_0(1370)$ and $f_0(1500)$ contributed in this best fit with $(11 \pm 2)$ % and $(10 \pm 2)$ %, the $f_2'(1525)$ and $f_2(1870)$ with $(15^{+1}_{-3})$ % and $(17 \pm 3)$ %, the $a_0(980)$ and $a_0(1450)$ with $(12 \pm 2)$ % and $(11 \pm 2)$ % and the $a_2(1320)$ contributed with $(25 \pm 4)$ %.

We then added an $f_0(1710)$, again parametrised as Breit-Wigner amplitude with fixed mass and width. However, this fit ($S = -8474$) resulted in unphysical $T$-matrix pole parameters out of phase space for the upper pole of the $(\eta\eta)_D-$wave: $m = 2150$ MeV and an unreasonable $\Gamma = 2$ MeV. There were several different solutions with almost identical $S$, all with an unreasonably narrow upper pole. Therefore, the conclusion was drawn that the $f_0(1710)$ is not required to describe the $\pi^0\eta\eta$ data set. To obtain an upper limit on the contribution of the $f_0(1710)$ the $K$-matrix pole parameters of the $(\eta\eta)_D-$wave were fixed to the values from the previous fit. The upper limit for the contribution of the $f_0(1710)$ to $\pi^0\eta\eta$ was 2.1 % at 90 % confidence level.

The parametrisation of the $(\eta\eta)_D-$wave with three poles in order to search for the $f_2(1565)$ decaying into $\eta\eta$ was not successful. These fits gave neither a significant improvement nor stable solutions and were therefore discarded.

The $\pi^0\eta\eta$ data are not sensitive to the precise mass of the $a_0(1450)$. Free parameters for the $a_0(1450)$ led to unphysical values. Replacing the $a_0(1450)$ by the $a_0(1300)$ with $K$-matrix parameters from $\pi^0\pi^0\eta$ led to an equally good fit.

## 7 Coupled Fit of $\overline{p}p \to \pi^0\pi^0\pi^0$ and $\overline{p}p \to \pi^0\eta\eta$

The analyses of $\pi^0\pi^0\pi^0$ and $\pi^0\eta\eta$ showed that both data sets required a high-mass isoscalar tensor state. Therefore the data sets were simultaneously fitted with a common description of the $f_2(1870)$. For $\pi^0\pi^0\eta$ the $f_2(1870)$ lies far above the phase space limit.

In order to use the full $\pi^0\pi^0\pi^0$ data sample and to give approximately equal weight to both data sets $S$ was rescaled by the number of events:

$$S' \;=\; S(\pi^0\pi^0\pi^0) \cdot \frac{N_{\pi^0\eta\eta}}{N_{\pi^0\pi^0\pi^0}} \;+\; S(\pi^0\eta\eta)\;. \qquad (11)$$

For the coupled fit of $\overline{p}p \to \pi^0\pi^0\pi^0$ and $\overline{p}p \to \pi^0\eta\eta$ the $(\pi\pi)_D-$wave and the $(\eta\eta)_D-$wave were combined and parametrised as a single $(2 \times 2)$ $K$-matrix with couplings to $\pi\pi$ and $\eta\eta$ and four poles, corresponding to the $f_2(1270)$, $f_2'(1525)$, $f_2(1565)$ and $f_2(1870)$. As the decay branching fractions of the $f_2(1270)$ and $f_2(1565)$ to $\eta\eta$ are very small compared to the decay into $\pi\pi$ [2], these couplings were set to zero. As the decay of the $f_2'(1525)$ into $\pi\pi$ compared to $\eta\eta$ is suppressed by a factor of 12 [2], the coupling of $f_2'(1525)$ to $\pi\pi$ was also set to zero. This reduced the number of free parameters and lead to a better convergence of the fit. The $f_2(1870)$ was allowed to decay into both $\pi^0\pi^0$ and $\eta\eta$. The $(3 \times 3)$ $K$-matrix parametrisation for the $(\pi\pi)_S/(\eta\eta)_S-$wave contained the $f_0(600)$, $f_0(980)$, $f_0(1370)$ and $f_0(1500)$.

The absolute ratio of the production strengths $\alpha_l^{J^{PC}}$ of resonances observed in both data sets should be independent of the final state in which they are observed. This was used to reduce the number of free parameters. Therefore, the production strengths of the isoscalar resonances in the two data sets were related:

$$|\alpha_l^{J^{PC}}(\pi^0\eta\eta)| = f \cdot |\alpha_l^{J^{PC}}(\pi^0\pi^0\pi^0)| \qquad (12)$$

where the parameters $f$ were determined by the fit. They differ for scalar and tensor resonances. It is not possible to relate the phases of the $\alpha_l^{J^{PC}}$ since interferences or rescattering effects can be different in the two final states. The number of parameters was thus reduced by 17. With 7 fitted parameters for the upper $K$-matrix poles of the $(\pi\pi)_D/(\eta\eta)_D-$wave corresponding to the $f_2'(1525)$, $f_2(1565)$ and $f_2(1870)$ the fit had 180 free parameters to determine. The coupled fit converged to a combined $S' = -20'013$ ($S(\pi^0\pi^0\pi^0) = -434'650$ and $S(\pi^0\eta\eta) = -8380$). The values from the separate fits were $-435'491$ and $-8393$, respectively. The slightly worse $S$ is due to the combined description of the isoscalar $S-$ and $D-$waves eqn. (12). The Dalitz plots and the projections for the two data sets differ only marginally from the ones obtained by the single fits. The $K$-matrix parameters and the corresponding $T$-matrix pole parameters of the isoscalar $D-$wave are listed in Table 5. All these parameters are compatible with the values found in the separate analyses; the masses were stable, the width of the $f_2(1565)$ decreased from 147 MeV to 113 MeV while the $f_2(1870)$ broadened somewhat to 385 MeV. The $f_2'(1525)$ and the $f_2(1565)$ are compatible with the PDG states [2]. The contributions of all resonances to the two data sets are compiled in Table 6. The contributions from the various partial waves remained reasonably stable.

| | $m_\alpha$ [ MeV ] | $\widetilde{\Gamma}_{\alpha,\pi\pi}$ [ MeV ] | $\widetilde{\Gamma}_{\alpha,\eta\eta}$ [ MeV ] | sheet III $(--)$ [ MeV ] | |
|---|---|---|---|---|---|
| $f_2(1270)$ | 1245 | 185 | | 1275 | 185 |
| $f_2'(1525)$ | $1505 \pm 10$ | | $80 \pm 10$ | $1508 \pm 9$ | $79 \pm 8$ |
| $f_2(1565)$ | $1556 \pm 10$ | $109 \pm 10$ | | $1552 \pm 13$ | $113 \pm 23$ |
| $f_2(1870)$ | $1914 \pm 40$ | $143 \pm 30$ | $221 \pm 30$ | $1867 \pm 46$ | $385 \pm 58$ |

**Table 5.** $K$-matrix parameters and $T$-matrix pole parameters in the relevant Riemann sheet III of the $(\pi\pi)_D$ and $(\eta\eta)_D$ −waves of the coupled fit. The $f_2(1270)$ parameters were fixed. The sheets are numbered according to the signs of the imaginary part of the break-up momenta for the decays into $\pi\pi$ and $\eta\eta$.

| | $\overline{p}p$ partial wave | $0^{-+}$ | $1^{++}$ | $2^{-+}$ | $2^{++}$ | $3^{++}$ | $\sum$ |
|---|---|---|---|---|---|---|---|
| $\pi^0\pi^0\pi^0$ | $(\pi\pi)_S\ \pi^0$ | 9 | 3 | 3 | | 3 | $18 \pm 3$ |
| | $f_0(1500)\ \pi^0$ | 5 | 2 | 1 | | 1 | $8 \pm 3$ |
| | $f_2(1270)\ \pi^0$ | 1 | 3 | 12 | 12 | 25 | $53 \pm 5$ |
| | $f_2(1565)\ \pi^0$ | 1 | 1 | 5 | 4 | 1 | $11 \pm 3$ |
| | $f_2(1870)\ \pi^0$ | 0 | 1 | 3 | 2 | 4 | $10 \pm 3$ |
| | $\sum$ | 17 | 9 | 26 | 11 | 38 | 100 |
| $\pi^0\eta\eta$ | $f_0(1370)\ \pi^0$ | 3 | 3 | 1 | | 2 | $8 \pm 2$ |
| | $f_0(1500)\ \pi^0$ | 7 | 2 | 1 | | 1 | $11 \pm 2$ |
| | $f_2'(1525)\ \pi^0$ | 2 | 2 | 8 | 1 | 3 | $15\ ^{+\ 1}_{-\ 3}$ |
| | $f_2(1870)\ \pi^0$ | 1 | 2 | 4 | 5 | 4 | $16 \pm 3$ |
| | $a_0(980)\ \eta$ | 8 | 1 | 1 | | 1 | $14 \pm 2$ |
| | $a_0(1450)\ \eta$ | 8 | 1 | 1 | | 0 | $11 \pm 2$ |
| | $a_2(1320)\ \eta$ | 1 | 2 | 12 | 7 | 3 | $25 \pm 4$ |
| | $\sum$ | 27 | 16 | 32 | 9 | 17 | 100 |

**Table 6.** Contributions (in %) to $\pi^0\pi^0\pi^0$ and $\pi^0\eta\eta$ from the coupled fit. $(\pi\pi)_S$ includes contributions from $f_0(600)$, $f_0(980)$ and $f_0(1370)$ which cannot be disentangled due to interferences.

Again we tried to include the $f_0(1710)$ into the coupled fit which was parametrised as a Breit-Wigner amplitude with mass 1715 MeV and width 125 MeV [2] and decaying into $\pi^0\pi^0$ and $\eta\eta$. This fit converged to a combined $S'$ of $-20'113$ ($S(\pi^0\pi^0\pi^0) = -435'648$ and $S(\pi^0\eta\eta) = -8453$) with a contribution of the $f_0(1710)$ of $(1.5 \pm 0.5)$ % and $(3.0 \pm 0.5)$ % to $\pi^0\pi^0\pi^0$ or $\pi^0\eta\eta$, respectively, but there were several solutions with almost the same log-likelihood. When the $f_0(1710)$ parameters were fitted, the convergence of the fit was very poor. The mass and width of the $f_0(1710)$ were then 1741 MeV and 265 MeV, respectively. However, the $f_2(1870)$ was pushed far out of phase space ($m = 2230$ MeV) and the width got unphysically small ($\Gamma = 25$ MeV). This fit was discarded.

Since the coupled fit without $f_0(1710)$ gave a good description of the two data sets and as the fits including the $f_0(1710)$ were not stable, pushing the upper pole of the $(\pi\pi)_D/(\eta\eta)_D$ −wave far out of phase space, the conclusion was drawn that the $f_0(1710)$ is definitely not required to describe the $\pi^0\pi^0\pi^0$ and $\pi^0\eta\eta$ data sets. From the fit with fixed masses and widths we derive an upper limit of the contribution of the $f_0(1710)$ to $\pi^0\pi^0\pi^0$ and $\pi^0\eta\eta$ of 2.1 % and 2.6 %, respectively, at 90 % confidence level and with $m = 1715$ MeV, $\Gamma = 125$ MeV [2].

## 8 Discussion

### 8.1 $(\pi\pi)_S$ −wave

The partial wave analysis showed that the $(\pi\pi)_S/(\eta\eta)_S$ − intensity in the three data sets could be described by the $(3 \times 3)$ four-pole $K$-matrix parametrisation with couplings to $\pi\pi$, $K\bar{K}$ and $\eta\eta$, which was derived in the coupled channel analysis at rest [1]. The relative strength of the $f_0(1500)$ decaying into $\eta\eta$ and $\pi^0\pi^0$ is in the present analysis

$$\frac{B(f_0(1500) \to \eta\eta)}{B(f_0(1500) \to \pi^0\pi^0)} = 0.24 \pm 0.10\,. \qquad (13)$$

This result is smaller but compatible with the value found in the coupled channel analysis at rest of $0.47 \pm 0.18$ using $B(\overline{p}p \to \pi^0 f_0(1500) \to \pi^0\pi^0\pi^0) = (1.27 \pm 0.33) \times 10^{-3}$, $B(\overline{p}p \to \pi^0 f_0(1500) \to \pi^0\eta\eta) = (0.60 \pm 0.17) \times 10^{-3}$ [1].

### 8.2 $f_0(1710)$ and $f_2(1710)$

The partial wave analyses of both $\pi^0\pi^0\pi^0$ and $\pi^0\eta\eta$ showed no evidence for an $f_2(1710)$. None of the fits had stable

solutions with an isoscalar tensor with this mass. The required tensor resonances were all distinctly different: the $\pi^0\eta\eta$ data required two tensor resonances, the $f_2'(1525)$ and a broad $f_2(1870)$ with $(1820^{+57}_{-10})$ MeV and $(358 \pm 42)$ MeV. In the description of the $\pi^0\pi^0\pi^0$ data, the $f_2(1270)$ was the dominant contribution. The second pole in the $(\pi\pi)_D-$wave is not a candidate for the $f_2(1710)$ since the $T$-matrix pole parameters of $m = (1554 \pm 12)$ MeV and $\Gamma = (147 \pm 27)$ MeV agree well with the $f_2(1565)$ [2]. Again, the $\pi^0\pi^0\pi^0$ data required a broad, high-mass tensor, the $f_2(1870)$, with $(1877 \pm 30)$ MeV and $(318 \pm 55)$ MeV. The coupled fit of $\pi^0\pi^0\pi^0$ and $\pi^0\eta\eta$ confirmed the $f_2(1870)$ and gave no indication for a $f_2(1710)$ either.

The fits of $\pi^0\pi^0\pi^0$ and $\pi^0\eta\eta$ including an $f_0(1710)$ were not satisfactory. In the best fit of $\overline{p}p \to \pi^0\pi^0\pi^0$ the improvement of the log-likelihood was not significant when the $f_0(1710)$ was included with the PDG mass of $m = 1715$ MeV and width $\Gamma = 125$ MeV [2]. Fits including the $f_0(1710)$ pushed the high-mass pole of the $(\pi\pi)_D-$wave far out of phase space. As soon as the $f_0(1710)$ was introduced into the best fit of $\overline{p}p \to \pi^0\eta\eta$, the high-mass pole of the $(\eta\eta)_D-$wave was pushed far out of phase and it became extremely narrow (about 10 MeV) and with a large contribution of 20 %. Fits with the $f_0(1710)$ but without the $f_2(1870)$ (even though both data sets clearly required the $f_2(1870)$) gave unphysical solutions. When mass and width of the $f_0(1710)$ were fitted freely, the resulting object was always broader than 250 MeV, led to strong interferences and the other resonances became unstable. The coupled fits to $\pi^0\pi^0\pi^0$ and $\pi^0\eta\eta$ showed basically the same behaviour.

The conclusion was drawn that the $f_0(1710)$ is not present in the $\pi^0\pi^0\pi^0$ and $\pi^0\eta\eta$ data sets from $\overline{p}p$ annihilation in flight at 900 MeV/$c$. The upper limit on the production and decay of the $f_0(1710)$ in $\overline{p}p \to \pi^0\pi^0\pi^0$ and $\overline{p}p \to \pi^0\eta\eta$ relative to that of the $f_0(1500)$ were calculated. With the upper limits for the contributions of the $f_0(1710)$ to $\pi^0\pi^0\pi^0$ and $\pi^0\eta\eta$ derived from the coupled fit, we obtained the 90 % confidence level upper limits

$$\frac{B(\overline{p}p \to \pi^0 f_0(1710) \to \pi^0\pi^0\pi^0)}{B(\overline{p}p \to \pi^0 f_0(1500) \to \pi^0\pi^0\pi^0)} < 0.31 \qquad (14)$$

$$\frac{B(\overline{p}p \to \pi^0 f_0(1710) \to \pi^0\eta\eta)}{B(\overline{p}p \to \pi^0 f_0(1500) \to \pi^0\eta\eta)} < 0.25\,, \qquad (15)$$

for $\overline{p}p$ annihilation at 900 MeV/c, assuming for the $f_0(1710)$ $m = 1715$ and $\Gamma = 125$ MeV [2].

In the limit of ideal mixing, and assuming no $s$-quark admixture in the proton wave-function, the OZI rule forbids the production of pure $s\bar{s}$ states in $\overline{p}p$ annihilation. It is known, however, that the $s\bar{s}$ mesons $\phi$ and $f_2'(1525)$ are enhanced in various channels of $\bar{p}p$ annihilation (see section 8.3), apparently violating the OZI rule. However, mainly $u\bar{u} + d\bar{d}$ scalar mesons are not suppressed in $\bar{p}p$ annihilation. The fact that the $f_0(1710)$ is not observed in $\overline{p}p$ annihilation in flight is therefore compatible with an $s\bar{s}$ assignment to the $f_0(1710)$. Recent results from the WA102 Collaboration [28] show that the ratio of branching ratios of the $f_0(1710)$ to $K\bar{K}$ and $\pi\pi$ is very large which points to a $s\bar{s}$ interpretation of the $f_0(1710)$, too. In refs. [29,30] the $f_0(1710)$ is the (mainly) $s\bar{s}$ member of the scalar ground state nonet with a small admixture of glue, while $f_0(1500)$ is mainly gluonic with a small admixture of quark-antiquark pairs.

### 8.3 $f_2'(1525)$

The partial wave analysis of $\pi^0\eta\eta$ showed that the $f_2'(1525)$ is definitely required to describe the data satisfactorily. The $T$-matrix parameters for the $f_2'(1525)$ from the coupled fit agree well with PDG values [2].

The Quark Line Rule states that the production of neutral resonances in $\overline{p}p$ annihilation occurs through the $u\bar{u}$ or $d\bar{d}$ part of the wave-function. The ratio of the production rates of the two isoscalar members is related to the mixing angle in the corresponding nonet. For the tensor mesons $f_2(1270)$ and $f_2'(1525)$ this ratio is

$$R = \frac{B(\overline{p}p \to f_2'(1525)\pi^0)}{B(\overline{p}p \to f_2(1270)\pi^0)} = \frac{\rho_{f_2'}}{\rho_{f_2}} \tan^2(\theta_{2^{++}} - \theta_{id}), \quad (16)$$

where $\theta_{2^{++}}$ denotes the mixing angle of the $2^{++}$ nonet. For ideal mixing $\theta_{id} = 35.3°$. For the phase space we use the Vandermeulen factor [31]:

$$\rho = q \exp\{A\sqrt{s - (m_f + m_{\pi^0})^2}\}, \qquad (17)$$

where $q$ is the break-up momentum, $m_f$ the mass of the resonance $\sqrt{s} = 2049.5$ MeV and $A = -0.83$ GeV$^{-1}$ [32]. The ratio of the two branching fractions

$$\frac{B(\overline{p}p \to f_2'(1525)\pi^0)}{B(\overline{p}p \to f_2(1270)\pi^0)} = 0.13 \pm 0.05\,, \qquad (18)$$

determined here was already corrected for the unseen decays of the $f_2(1270)$ and $f_2'(1525)$. Using $\theta_{2^{++}} = (25.3 \pm 1.1)°$ from Crystal Barrel data [33] we find $R = 0.025 \pm 0.007$, which is significantly smaller than the measured value of eqn. (18). The contribution of the $f_2'(1525)$ stems mainly from high angular momentum states (Table 6). A large and compatible value of $R$ was reported by the Obelix Collaboration in $\overline{p}p$ annihilation at rest in gaseous hydrogen [34] where initial $P-$wave contributions are large. The present measurement confirms the large violation of the OZI rule for tensor meson production in $\overline{p}p$ annihilation from higher $\overline{p}p$ initial states (for a review see e.g. ref. [7]).

### 8.4 $f_2(1565)$

The best fit to the $\pi^0\pi^0\pi^0$ data set was obtained including the $f_2(1565)$ in the $K$-matrix parametrisation of the $(\pi\pi)_D-$wave. The coupled fit of $\pi^0\pi^0\pi^0$ and $\pi^0\eta\eta$ gave a contribution of the $f_2(1565)$ to $\pi^0\pi^0\pi^0$ of $(11 \pm 3)$ %. The $T$-matrix pole parameters for the $f_2(1565)$ from the coupled fit agree well with the PDG values. The relative

ratio of production in $\overline{p}p$ annihilation at 900 MeV/$c$ and decay to $\pi^0\pi^0$ for the $f_2(1270)$ and $f_2(1565)$ is:

$$\frac{B(\overline{p}p \to \pi^0 f_2(1565) \to \pi^0\pi^0\pi^0)}{B(\overline{p}p \to \pi^0 f_2(1270) \to \pi^0\pi^0\pi^0)} = 0.21 \pm 0.06\,. \quad (19)$$

The result (19) is in good agreement with the value found in the analysis at rest, $0.27 \pm 0.10$ [35].

In the current analysis only the decay of the $f_2(1565)$ into $\pi\pi$ was allowed since no significant contribution of the $f_2(1565)$ to $\pi^0\eta\eta$ was found. As the $f_2(1565)$ is very close to the $f_2'(1525)$ it was not possible to disentangle the contribution of the $f_2(1565)$; therefore no upper limit for $B(f_2(1565) \to \eta\eta)$ can be given.

### 8.5 $f_2(1870)$

The $\pi^0\pi^0\pi^0$ and $\pi^0\eta\eta$ data sets clearly require a high-mass tensor $f_2(1870)$ decaying to $\pi^0\pi^0$ or $\eta\eta$. It is unlikely that the $f_2(1870)$ is the same state as the $f_2(1810)$ decaying into $\pi\pi$ [2] since mass and width do not agree, e.g. the latter is much narrower. Hence we cannot confirm the $f_2(1810)$. On the other hand, the $f_2(1870)$ is not incompatible with the $f_2(1950)$ (decaying into $4\pi$ [36] and possibly into $K^*\overline{K}^*$ [37]). The width of the $f_2(1870)$ is compatible with the width of the $f_2(1950)$ of $(400-500)$ MeV [2]. Its mass, $m = (1960 \pm 30)$ MeV, is somewhat higher than the one determined in this analysis.

The relative strength of the $f_2(1870)$ decaying to $\eta\eta$ and $\pi^0\pi^0$ is

$$\frac{B(f_2(1870) \to \eta\eta)}{B(f_2(1870) \to \pi^0\pi^0)} = 0.27 \pm 0.10\,, \quad (20)$$

The branching fractions are related to the ratio of couplings via

$$\frac{\gamma^2(f_2 \to \eta\eta)}{\gamma^2(f_2 \to \pi\pi)} = \frac{1}{3}\frac{B(\overline{p}p \to f_2\pi^0, f_2 \to \eta\eta)}{B(\overline{p}p \to f_2\pi^0, f_2 \to \pi^0\pi^0)}\,\frac{q_{\pi\pi}}{q_{\eta\eta}}\,\frac{F_{\pi\pi}}{F_{\eta\eta}}\,, \quad (21)$$

where $F$ is a form factor e.g. [38]:

$$F(q) = q^{2l}\exp\{-q^2/8\beta^2\}\,. \quad (22)$$

The factor 3 in the denominator of eqn. (21) accounts for the three charge combinations $\pi^0\pi^0$, $\pi^+\pi^-$ and $\pi^-\pi^+$. With $l = 2$, $\beta = 0.4$ GeV/$c$ [38] and the break-up momenta $q_{\pi\pi} = 0.925$ GeV/$c$ and $q_{\eta\eta} = 0.758$ GeV/$c$ one obtains

$$\frac{\gamma^2(f_2(1870) \to \eta\eta)}{\gamma^2(f_2(1870) \to \pi\pi)} = 0.20 \pm 0.07\,. \quad (23)$$

This ratio is related to $SU(3)$ mixing angles. For a quarkonium state $|\,Q\bar{Q}\,\rangle$ we have

$$|\,Q\bar{Q}\,\rangle = \cos\alpha\,|\,n\bar{n}\,\rangle - \sin\alpha\,|\,s\bar{s}\,\rangle \quad (24)$$

while

$$|\,\eta\,\rangle = \cos\phi\,|\,n\bar{n}\,\rangle - \sin\phi\,|\,s\bar{s}\,\rangle\,, \quad (25)$$

where $n\bar{n} \equiv (u\bar{u} + d\bar{d})/\sqrt{2}$. The mixing angles $\alpha$ and $\phi$ are related to the usual nonet mixing angle $\theta$ [2] by the relation $\alpha = 54.7^\circ + \theta$, $\phi = 54.7^\circ + \theta_{PS} = (37.4 \pm 1.8)^\circ$ [32], where $\theta_{PS}$ is the mixing angle for the pseudoscalar mesons. The ratio of couplings then becomes [29]:

$$\frac{\gamma^2(Q\bar{Q} \to \eta\eta)}{\gamma^2(Q\bar{Q} \to \pi\pi)} = \frac{1}{3}\left[\cos^2\phi - \sqrt{2}\tan\alpha\sin^2\phi\right]^2\,. \quad (26)$$

With the result (23) one gets two solutions for the mixing angle $\alpha$:

$$\begin{array}{l}\alpha_1 = (\ \ 69.6\,^{+\ 1.6}_{+\ 2.2}\,)^\circ \\ \alpha_2 = (-15.4\,^{+\ 16.1}_{-\ 11.9}\,)^\circ\end{array}\,. \quad (27)$$

The second solution $\alpha_2$ is compatible with $\alpha = 0^\circ$, therefore ideal mixing. The $f_2(1870)$ would then be a state with a dominant $n\bar{n}$ component, hence a $2^{++}$ radial excitation of the $f_2(1270)$. The ambiguity between $\alpha_1$ and $\alpha_2$ could be solved by measuring the $\eta\eta'$ and/or $K\bar{K}$ decay rates of the $f_2(1870)$.

### 8.6 $(\pi\eta)_S-$wave

The partial wave analysis of $\pi^0\pi^0\eta$ showed a significant improvement when the $K$-matrix parameters of the second pole of the $(\pi\eta)_S-$wave, the $a_0(1450)$, were fitted freely, resulting in a $a_0(1300)$. Eventhough the improvement of the log-likelihood was significant we do not view this as strong evidence for an $a_0(1300)$. As the $a_2(1320)$ contributes more than 30 % to the $\pi^0\pi^0\eta$ data set it is possible that the fit compensates for a slightly inadequate description of the $a_2(1320)$. For example the inclusion of $J = 4$ initial states improves the description of the $a_2(1320)$ lineshape. Even though the total contribution of all $J = 4$ initial states was less than 3 %, the contribution of the $a_0(1300)$ then dropped from 7 % to 4 %. Therefore, the possibility cannot be ruled out that the $a_0(1300)$ is just an artifact.

Since the fits were less stable with the $a_0(1300)$, and as the parameters of the other resonances were not sensitive to the exact shape of the $(\pi\eta)_S-$wave in $\pi^0\eta\eta$, the results for $\overline{p}p \to \pi^0\eta\eta$ are quoted from the fit with the $a_0(1450)$.

### 8.7 $a_2(1660)$

The analysis of $\overline{p}p \to \pi^0\pi^0\eta$ clearly showed that the $(\pi\eta)_D-$wave requires two poles, corresponding to the $a_2(1320)$ and $a_2(1660)$, to describe the data set satisfactorily. The $T$-matrix pole parameters for the $a_2(1660)$ were $m = (1698 \pm 44)$ MeV and $\Gamma = (265 \pm 55)$ MeV, which agree well with the Breit-Wigner parameters determined in the Crystal Barrel analysis of $\pi^0\eta\eta$ at 1940 MeV/$c$ ($m = (1660 \pm 40)$ MeV and $\Gamma = (280 \pm 70)$ MeV [9]). The present

result is the first clear evidence for the $a_2(1660)$ in the $\pi^0\pi^0\eta$ final state. The L3 collaboration analysing $\gamma\gamma \to \pi^+\pi^-\pi^0$ [10] also reported a $2^{++}$ isovector state with mass of $(1752 \pm 21 \pm 4)$ MeV and a width $(150 \pm 110 \pm 34)$ MeV decaying into $\pi^+\pi^-\pi^0$.

## 9 Conclusions

We have analysed the three final states $\pi^0\pi^0\pi^0$, $\pi^0\pi^0\eta$ and $\pi^0\eta\eta$ in $\overline{p}p$ annihilation at 900 MeV/$c$ using the $K$-matrix and helicity formalisms. A coupled fit of $\pi^0\pi^0\pi^0$ and $\pi^0\eta\eta$ was performed using the maximum likelihood method. In the analyses of $\pi^0\eta\eta$ and $\pi^0\pi^0\pi^0$ a $2^{++}$ isoscalar state was found with mass $(1867 \pm 46)$ MeV and width $(385 \pm 58)$ MeV decaying to $\eta\eta$ and $\pi^0\pi^0$, compatible with a dominant $u\bar{u} + d\bar{d}$ content. The strong signal from the $f_2'(1525)$ observed in $\pi^0\eta\eta$ violates the OZI rule in $\overline{p}p$ annihilation from higher angular momentum states. The $f_2(1565)$, seen so far only at rest, is observed in the $\pi^0\pi^0\pi^0$ channel. In the analyses of $\pi^0\pi^0\pi^0$ and $\pi^0\eta\eta$ no signal for the $f_0(1710)$ was observed. As the Quark Line Rule suppresses the production of $s\bar{s}$ states in $\overline{p}p$ annihilation, this non-observation is consistent with a large $s\bar{s}$ content of the $f_0(1710)$. The analysis of $\overline{p}p \to \pi^0\pi^0\eta$ revealed a tensor resonance with isospin one with mass $(1698 \pm 44)$ MeV and width $(265 \pm 55)$ MeV decaying into $\pi^0\eta$. This state coincides with the $a_2(1660)$ observed in the Crystal Barrel analysis of $\pi^0\eta\eta$ at 1940 MeV/$c$. Our $\pi^0\pi^0\eta$ data show a slight preference for an $a_0(1300)$, with a mass of $1236 \pm 10$ MeV and a width of $81 \pm 21$ MeV, over $a_0(1450)$. However, this may be due to a truncation of the initial angular momentum states, leading to an imperfect description of the $a_2(1320)$ region.

## Acknowledgements

We would like to thank the technical staff of the LEAR machine group and all the participating institutions for their invaluable contributions to the success of the experiment. We also thank the staff of the CSCS in Manno, Switzerland, for their help in porting the program and the use of the SX-5. We acknowledge financial support from the German Bundesministerium für Bildung, Wissenschaft, Forschung und Technologie, the Schweizerischer Nationalfonds, the British Particle Physics and Astronomy Research Council, the U.S. Department of Energy and the National Science Research Fund Committee of Hungary (contract No. DE−FG03−87ER40323, DE−AC03−76SF00098, DE−FG02−87ER40315 and OTKA T023635). K. M. Crowe and F.-H. Heinsius acknowledge support from the A. von Humboldt Foundation.

## References

1. C. Amsler et al., Phys. Lett. **B355**(1995) 425
2. D. E. Groom et al., Review of Particle Physics, Eur. Phys. J. **C15**(2000) 1
3. A. Abele et al., Phys. Rev. **D57**(1998) 3860
4. A. Bertin et al., Phys. Lett. **B434**(1998) 180
5. J. Z. Bai et al., Phys. Lett. **B472**(2000) 207
6. B. French et al., Phys. Lett. **B460**(1999) 213
   D. Barberis et al., Phys. Lett. **B462**(1999) 462
7. C. Amsler, Rev. Mod. Phys. **70**(1998) 1293
8. B. May et al., Phys. Lett. **B225**(1989) 450
9. A. Abele et al., Eur. Phys. J. **C8**(1999) 67
10. M. Acciarri et al., Phys. Lett. **B413**(1997) 147
11. E. Aker et al., Nucl. Instr. Meth. **A321**(1992) 69
12. A. V. Anisovich et al., Phys. Lett. **B449**(1999) 154
    A. V. Anisovich et al., Phys. Lett. **B452**(1999) 180
13. C. Amsler et al., Phys. Lett. **B311**(1993) 362
14. C. Amsler et al., Phys. Lett. **B342**(1995) 433
15. C. Amsler et al., Phys. Lett. **B333**(1994) 277
16. C. Amsler et al., Phys. Lett. **B353**(1995) 571
17. M. Jacob, G. C. Wick, Ann. Phys. (NY) **7**(1959) 404
18. D. Herndorn, P. Söding and R. J. Cashmore, Phys. Rev. **D11**(1975) 3165
19. I. J. R. Aitchison, Nucl. Phys. **A189**(1972) 417
20. S. U. Chung et al., Ann. Physik **4**(1995) 404
21. F. v. Hippel und C. Quigg, Phys. Rev. **D5**(1972) 624
22. C. J. Batty, Nucl. Phys. **A601**(1996) 425
23. J. Lüdemann, PhD thesis, Ruhr-Universität Bochum, 1995
24. S. Bischoff, PhD thesis, Universität Karlsruhe, 1999
25. M. Heinzelmann, PhD thesis, Universität Zürich, 2000
26. F. James, CERN Program Library Long Writeup D506 (1994)
27. see http://www.cscs.ch/
28. D. Barberis et al., Phys. Lett. **B462**(1999) 462
29. C. Amsler and F. E. Close, Phys. Rev. **D53**(1996) 295
30. F. E. Close and A. Kirk, Phys. Lett. **B483**(2000) 345
31. J. Vandermeulen, Z. Phys. **C37**(1988) 563
32. C. Amsler et al., Phys. Lett. **B294**(1992) 451
33. A. Abele et al., Phys. Lett. **B385**(1996) 425
34. A. Alberico et al., Phys. Lett. **B438**(1998) 430
35. A. Abele et al., Nucl. Phys. **A609**(1996) 562
36. D. Barberis et al., Phys. Lett. **B413**(1997) 217
37. D. Aston et al., Nucl. Phys. **B21**(1991) 5 (suppl)
38. S. Godfrey and N. Isgur, Phys. Rev. **D32**(1985) 189